

Pharmacometrics-Enabled DOse OPtimization (PEDOOP) for Seamless Phase I-II Trials in Oncology

Shijie Yuan*, Zhanbo Huang[†], Jiaxin Liu[‡], and Yuan Ji[§]

February 23, 2024

Abstract

We consider a dose-optimization design for first-in-human oncology trial that aims to identify a suitable dose for late-phase drug development. The proposed approach, called the Pharmacometrics-Enabled DOse OPtimization (PEDOOP) design, incorporates observed patient-level pharmacokinetics (PK) measurements and latent pharmacodynamics (PD) information for trial decision making and dose optimization. PEDOOP consists of two seamless phases. In phase I, patient-level time-course drug concentrations, derived PD effects, and the toxicity outcomes from patients are integrated into a statistical model to estimate the dose-toxicity response. A simple dose-finding design guides dose escalation in phase I. At the end of the phase I dose finding, a graduation rule is used to assess the safety and efficacy of all the doses and select those with promising efficacy and acceptable safety for a randomized comparison against a control arm in phase II. In phase II, patients are randomized to the selected doses based on a fixed or adaptive randomization ratio. At the end of phase II, an optimal biological dose (OBD) is selected for late-phase development. We conduct simulation studies to assess the PEDOOP design in comparison to an existing seamless design that also combines phases I and II in a single trial.

Keywords: Adaptive randomization; Dose finding; Optimal biological dose; Pharmacodynamics; Pharmacokinetics.

1 Introduction

Early-phase oncology trials like phase I and phase II studies investigate the toxicity and efficacy of a new drug. In most phase I trials, the goal is to explore the toxicity profile of the tested drug and identify the maximum tolerated

*Department of Statistics and Data Science, The University of Texas at Austin, Austin, USA

[†]School of Data Science, Fudan University, Shanghai, CHN

[‡]Cytel Inc., Shanghai, CHN

[§]Department of Public Health Sciences, The University of Chicago, Chicago, USA; Corresponding email: koaeraser@gmail.com

dose (MTD), the highest dose that does not cause unacceptable side effects. If a target toxicity rate p_T is specified in the trial, the MTD is defined as the highest dose with a toxicity probability less than p_T . A large number of designs have been proposed for phase I trials, ranging from model-free designs like the “3+3” design (Storer, 1989) and the “i3+3” design (Liu et al., 2020), model-based designs like the continual reassessment method (CRM) (O’Quigley et al., 1990), the mTPI design (Ji et al., 2010), the mTPI-2 designs (Guo et al., 2017), and the BOIN design (Liu and Yuan, 2015). Some model-based designs use independent likelihood and prior distributions, resulting in independent posterior inference across doses and algorithm-like decision rules. These designs (mTPI, mTPI-2, BOIN) are also referred to as model-assisted designs.

All the aforementioned designs are developed for cytotoxic drugs the toxicity and efficacy of which are assumed to increase with the dose level. In modern oncology drug development, novel therapeutics like kinase inhibitors, monoclonal antibodies, and immunology drugs behave differently from traditional cytotoxic agents in that efficacy may plateau or sometimes even decrease as dose level increases (US Food and Drug Administration, 2023). Consequently, MTD may no longer be optimal for patient care as a lower dose may be as potent but safer. Instead of finding the MTD, modern phase I studies are encouraged to identify the optimal biological dose (OBD) that balances the tradeoff between toxicity and efficacy. Ideally, OBD should be no higher than MTD. Apparently, the identification of the OBD is not achievable by only considering the dose-limiting toxicity (DLT) data from the phase I studies. Here we aim to propose a model to incorporate pharmacokinetics (PK), pharmacodynamics (PD) information, toxicity and efficacy outcomes of the tested drug in a seamless phase I-II trial for dose optimization. The proposed method, called PEDDOOP, is an attempt to respond to the FDA’s Project Optimus. Specifically, PEDDOOP aims to integrate pharmacological and clinical data to identify an OBD through dose escalation and randomized dose comparison. Even though PK and PD analyses are routinely performed in oncology dose-finding trials, they are not formally or quantitatively integrated with clinical data in a dose-finding design. In PEDDOOP, we model the time-course PK measurements of each patient and use a summary statistics like the maximum serum concentration or the area under the concentration-time curve (AUC) (Piantadosi and Liu, 1996; Patterson et al., 1999; Whitehead et al., 2001, 2007). Ursino et al. (2017) for integrative modeling. Specifically, the summary statistics of PK is used as a covariate in a logistic model for the toxicity outcome. We find that this improves the estimation of the toxicity probabilities across the doses.

Furthermore, PEDDOOP follows the idea in (Su et al., 2022) and derives a PD summary, which is subsequently linked to efficacy outcomes. Su et al. (2022) propose a semi-mechanistic dose-finding (SDF) design based on the modeling of PK and PD profiles and their effects on the DLT probability. A PK-enabled dose-finding model is developed by the authors to incorporate patient-level PK data into phase I. They use drug concentrations to model

a latent PD outcome, which are subsequently linked to DLT outcome. We modify the SDF design by assuming that the PD is associated to the efficacy of the new drug, rather than toxicity. In summary, PEDOOP consists of two modeling components: one for toxicity with PK as covariate, and the other for efficacy with PD as covariate. Both components are derived from the patient-level drug concentrations.

For trial design, we follow the idea in the SEARS design (Pan et al., 2014) that combines phase I dose escalation based on toxicity with phase II randomized dose comparison based on efficacy. This idea directly addresses some recommendations in the recent FDA’s draft guidance on oncology dose-finding trials. (US Food and Drug Administration, 2023)

A schema of PEDOOP is presented in Figure 1. We firstly calculate the DLT probability based on PK data and DLT outcomes, and conduct dose escalation using the CRM frame (O’Quigley et al., 1990). Then, once all efficacy outcomes are collected, graduation rules are used to select doses from all doses in phase I by considering PK data, DLT, and efficacy outcomes. Then, the adaptive randomization (AR) method is used to adjust the patient allocation ratio among the selected doses from phase I and an optional control arm during the simulated phase II trials. In the end, an OBD will be selected for further study, or the tested drug will be declared non-promising. We assume the patients in phase I are with different indications and those in phase II are restricted to a specific indication.

The remainder of the article is organized as follows. Sections 2 and 3 describe the phase I and phase II designs of PEDOOP, respectively. In Section 4, we conduct simulation studies to demonstrate the design performance of PEDOOP. We end the paper with a discussion in Section 5.

2 Phase I Design

The proposed PEDOOP design enrolls patients in cohorts, say three patients per cohort. After a cohort of patients is enrolled and treated at a dose, they are followed for a period of time for PK, toxicity, and efficacy outcomes. Specifically, PEDOOP models the DLT outcomes and time-series drug plasma concentration for each patient in phase I, and at the end of phase I, also models efficacy outcomes. In other words, three types of information for each patient are collected for PEDOOP in the phase I portion, the drug plasma concentrations over a fixed schedule, the binary toxicity outcome, and the binary efficacy outcome. Let X_{ij} denote the drug plasma concentration measured at time t_j for patient i , Y_i the binary toxicity outcome, and Z_i the binary efficacy outcome. Here $Y_i = 1$ represents patient i experiences the DLT after administered by the tested drug, and $Y_i = 0$ not. Similarly, $Z_i = 1$ represents patient i shows an efficacy response (such as objective response), and $Z_i = 0$ not. DLT outcomes are recorded for a period of time after drug administration, such as 21 or 28 days. Drug concentration is typically measured at

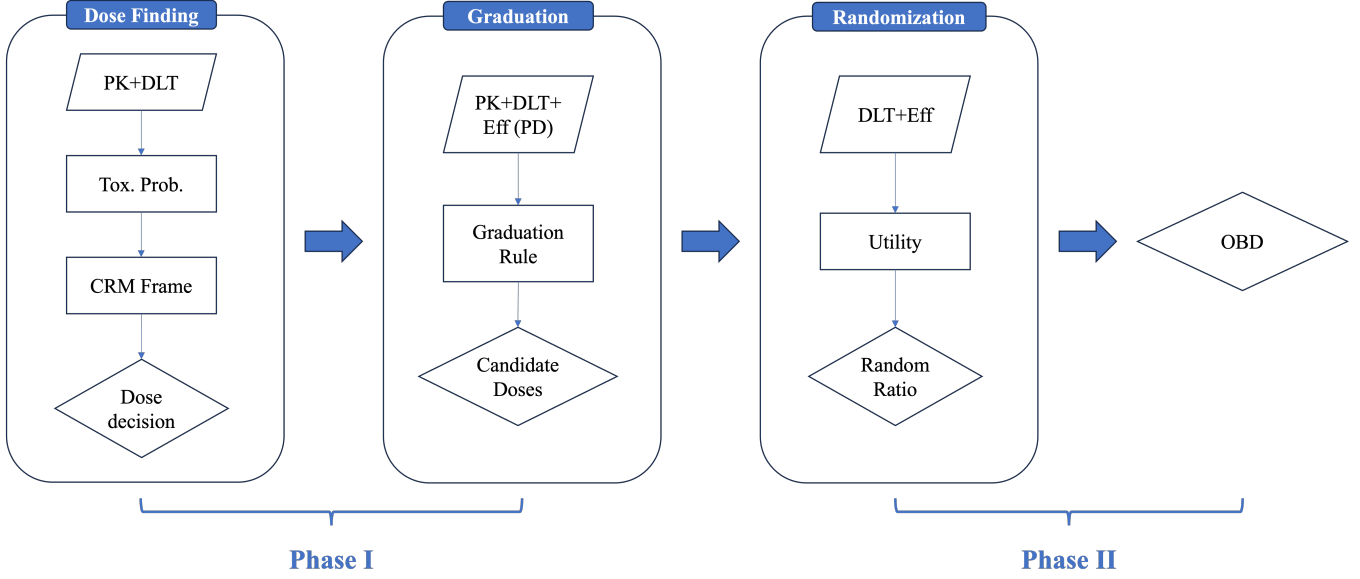


Figure 1: Schema of the PEDOOP design. In Phase I, a PK-enabled design guides dose finding and a graduation rule incorporates PK, DLT, and Efficacy (enhanced by PD) decides which doses are selected for randomized comparison. Phase II involves a randomized comparison of selected doses after which an OBD is selected.

fixed time points during the first week of drug administration. The efficacy outcome, however, takes much longer to measure, usually after 12 weeks of treatment. Therefore, we do not model efficacy data for making dose escalation decisions. Instead, efficacy data are used for selecting doses for randomized comparison. PEDOOP links X_{ij} , Y_i , and Z_i in a clever way, which will be introduced in Sections 2.2 and 2.3.

2.1 Drug Concentration

Let d_i denote the drug dosage administered to patient i , $d_i \in \{1, \dots, D\}$, where D is the total of tested doses. For simplicity, in this paper, we use a one-compartmental model (Shargel et al., 1999) for drug concentration over time, which assumes that the human body can be treated as a single homogeneous compartment. The model is popular in studies where drugs are administered through the intravenous (IV) injection. Denote by $c(t)$ the true drug concentration at time t . The first-order one-compartment model is given by

$$\frac{dc_i(t)}{dt} = -k_i t \text{ with an initial value } c_i(0) = \frac{d_i}{V_i}.$$

Solving the differential equation, we have

$$c_i(t \mid d_i, V_i, k_i) = \frac{d_i}{V_i} e^{-k_i t}. \quad (1)$$

Here, k_i and V_i are the patient-specific elimination rate and volume of distribution, respectively, and t is the time after the drug administration. In practice, $c(t)$ is measured with error and we denote X_{ij} the observed concentration at time t_j for patient i . We assume $\log(X_{ij}) = \log(c_i(t_j | d_i, V_i, k_i)) + \epsilon_{ij}$, where ϵ_{ij} is the random error. It is common to impose a normal distribution on ϵ_{ij} with mean 0 and standard deviation σ , i.e., $\epsilon_{ij} \sim N(0, \sigma^2)$. Therefore,

$$\log(X_{ij}) \sim N(\log(c_i(t_j | d_i, V_i, k_i)), \sigma^2).$$

In subsequent discussion, we will link PK with toxicity outcomes at each dose. This requires a summary of drug concentration across patients assigned to the same dose. To this end, we propose a prior distribution for V_i and k_i so that an average dose-level drug concentration can be computed by integrating them out. Specifically, let

$$k_i \sim \text{Gamma}(\alpha_k, \lambda_k), \quad V_i \sim \text{Gamma}(\alpha_V, \lambda_V) \quad (2)$$

Here, $\text{Gamma}(\alpha, \lambda)$ denotes a gamma distribution with the shape parameter of α and the rate parameter of λ . The prior distributions describe the variabilities associated with patients, as each individual physiological condition may vary. By integrating k_i and V_i over their prior distributions across patients assigned to the same dose, we derive the dose-level drug concentration at dose d as

$$\begin{aligned} c(t | d) &= \iint c(t | d, V, k) g_V(V) g_k(k) dV dk \\ &= \frac{d\lambda_V}{\alpha_V - 1} \left(\frac{\lambda_k}{\lambda_k + t} \right)^{\alpha_k} \end{aligned} \quad (3)$$

where $g_V(V)$ and $g_k(k)$ are the probability density functions of the prior distribution of V and k as per (2). We assume $\alpha_V > 1$ to ensure a positive value for $c(t | d)$.

2.2 Link PK and Toxicity

Using (1), we can easily obtain the AUC for patient i by integrating $c_i(t)$ from 0 to t_{ref} , a prespecified time, i.e.,

$$AUC(d_i, V_i, k_i; t_{ref}) = \int_0^{t_{ref}} c_i(t | d_i, V_i, k_i) dt = \frac{d_i}{V_i k_i} (1 - e^{-k_i t_{ref}})$$

By setting t_{ref} to infinity, we obtain the expected AUC for patient i as

$$AUC_i \equiv AUC(d_i, V_i, k_i; \infty) = \int_0^\infty c_i(t | d_i, V_i, k_i) dt = \frac{d_i}{V_i k_i}. \quad (4)$$

Similarly, we obtain the dose-level AUC for dose d by integrating V_i and k_i out of (4) over their prior distributions (2). Mathematically, this is equivalent to integrating (3) from 0 to the infinity. As a result, we derive the dose-level AUC for dose d via

$$AUC(d | \alpha_V, \lambda_V, \alpha_k, \lambda_k) = \int_0^\infty c(t | d) dt = \frac{d\lambda_V \lambda_k}{(\alpha_V - 1)(\alpha_k - 1)}. \quad (5)$$

We assume $\alpha_V > 1$ and $\alpha_k > 1$ to ensure a positive value for the AUC value. For simplicity, we let $\boldsymbol{\theta}_{\text{PK}} = (\alpha_V, \lambda_V, \alpha_k, \lambda_k)$ for notation purpose.

Finally, we assume a linear relationship between the logit of toxicity probability p_d and the logarithm of the AUC, given by

$$\text{logit}(p_d) = \text{logit}[p(d \mid \boldsymbol{\theta}_{\text{PK}})] = \beta_0 + \beta_1 \times \log[AUC(d \mid \boldsymbol{\theta}_{\text{PK}})]. \quad (6)$$

Denoting by Y_i the binary DLT outcome of patient i , we assume a binomial distribution

$$Y_i \sim \text{Binomial}(p(d_i \mid \boldsymbol{\theta}_{\text{PK}})).$$

2.3 Link PK, PD, and Efficacy

We now develop a new model that links PK to a latent PD and efficacy. [Su et al. \(2022\)](#) modeled a latent composite outcome to describe the relationship between the drug concentration and the pharmacologic effect. We follow their idea and model a latent composite PD outcome as a function of drug concentration at a steady state. We consider the sigmoid Emax model, a classic and widely used model in the PD analysis. Let $r(t \mid d)$ be the drug effect intensity between time t and $t + \Delta t$ when $\Delta t \rightarrow 0$, which is the intensity of drug at time t . Assume

$$r(t \mid d) = \frac{E_{\max} \times c(t \mid d)^\gamma}{ED_{50}^\gamma + c(t \mid d)^\gamma}, \quad (7)$$

where E_{\max} is the maximum possible drug effect, ED_{50} is the drug concentration that causes 50% of E_{\max} , and γ is an operational shape (also called ‘hill’) factor that allows a better data fit ([Meibohm and Derendorf, 1997](#); [Ting and Ting, 2006](#)). Similar to the toxicity model, by integrating $r(t \mid d)$ from 0 to infinity, we derive the cumulative effect of the drug for dose d , $\eta(d)$, given by

$$\begin{aligned} \eta(d) &= \int_0^\infty r(t \mid d) dt = \int_0^\infty \frac{E_{\max} \left(\frac{d\lambda_V \lambda_k^{\alpha_k}}{\alpha_V - 1} \right)^\gamma \left(\frac{1}{\lambda_k + t} \right)^{\gamma\alpha_k}}{ED_{50}^\gamma + \left(\frac{d\lambda_V \lambda_k^{\alpha_k}}{\alpha_V - 1} \right)^\gamma \left(\frac{1}{\lambda_k + t} \right)^{\gamma\alpha_k}} dt \\ &= \frac{E_{\max} \left(\frac{d\lambda_V \lambda_k^{\alpha_k}}{\alpha_V - 1} \right)^\gamma}{ED_{50}^\gamma} \int_0^\infty \frac{1}{(\lambda_k + t)^{\gamma\alpha_k} + \left(\frac{d\lambda_V \lambda_k^{\alpha_k}}{\alpha_V - 1} \right)^\gamma / ED_{50}^\gamma} dt \\ &\stackrel{x=\lambda_k+t}{=} C(d) E_{\max} \int_{\lambda_k}^\infty \frac{1}{x^{\gamma\alpha_k} + C(d)} dx \end{aligned} \quad (8)$$

where $C(d) = \left(\frac{d\lambda_V \lambda_k^{\alpha_k}}{\alpha_V - 1} \right)^\gamma / ED_{50}^\gamma$. For a given value of $\gamma * \alpha_k > 1$, there is a closed form for (8). Hereinafter, we denote $\phi = \gamma * \alpha_k$. For example, if we let $\phi = 2$, equation (8) becomes

$$\eta(d) = C(d) E_{\max} \times \frac{\arctan\left(\frac{x}{\sqrt{C(d)}}\right)}{\sqrt{C(d)}} \Big|_{\lambda_k}^\infty = \sqrt{C(d)} E_{\max} \left[\frac{\pi}{2} - \arctan\left(\frac{\lambda_k}{\sqrt{C(d)}}\right) \right].$$

The integration in (8) is solvable once ϕ is given. For mathematical simplicity, we assume a categorical prior distribution on ϕ , $\phi \sim \text{Cat}(4, \mathbf{p})$, where $\phi \in \{2, 3, 4, 5\}$ and $\mathbf{p} = (0.25, 0.25, 0.25, 0.25)$. See Appendix A for more details.

Next we choose a link function $h(\eta)$ to connect the efficacy probability and the PD drug effect. The link function should satisfy (Su et al., 2022)

1. $h(\eta) \in [0, 1]$
2. $h(\eta)$ is non-decreasing with respect to η
3. $h(0) = 0$ and $\lim_{\eta \rightarrow \infty} h(\eta) = 1$.

The first criterion means that the minimum of the efficacy probability is 0, and the maximum is 1. The second means that efficacy is non-decreasing with PD, and the third one means that when the PD effect of the drug reaches infinity or zero, the drug must be efficacious with probability one or zero, respectively. An example of the link function is $h(\eta) = 1 - \exp(-\eta)$ in Su et al. (2022), which is the one chosen here for PEDOOP. Therefore,

$$q_d \equiv q(d \mid \boldsymbol{\theta}_{\text{PK}}, E_{\text{max}}, ED_{50}, \phi) = 1 - \exp(-\eta(d)). \quad (9)$$

Here, q_d is the efficacy probability of dose d . Finally, denoting by Z_i the binary efficacy outcome of patient i , we assume

$$Z_i \sim \text{Binomial}(q(d_i \mid \boldsymbol{\theta}_{\text{PK}}, E_{\text{max}}, ED_{50}, \phi)).$$

2.4 Posterior Inference

Let $\boldsymbol{\theta}$ denote all the dose-level parameters in the model, i.e., $\boldsymbol{\theta} = (\alpha_V, \lambda_V, \alpha_k, \lambda_k, \sigma^2, \beta_0, \beta_1, ED_{\text{max}}, ED_{50}, \phi)$. Denote by $\mathcal{D}_I = \{(X_{ij}, Y_i, Z_i, d_i)\}$ all the available data from Phase I. The joint posterior distribution can be written as

$$\begin{aligned} \pi(\boldsymbol{\theta} \mid \mathcal{D}_I) &\propto \prod_i \prod_j \frac{1}{\sigma \sqrt{2\pi}} \exp\left(-\frac{(\log(X_{ij}) - \log(c_i(t_j \mid d_i, V_i, k_i)))^2}{2\sigma^2}\right) \times \prod_i f(V_i, k_i \mid \alpha_V, \lambda_V, \alpha_k, \lambda_k) \\ &\quad \times \prod_d q_d^{z_d} (1 - q_d)^{n_d - z_d} \\ &\quad \times \prod_d p_d^{y_d} (1 - p_d)^{n_d - y_d} \\ &\quad \times g(\boldsymbol{\theta}), \end{aligned} \quad (10)$$

where $n_d = \sum_i I(d_i = d)$, $y_d = \sum_i I(d_i = d, Y_i = 1)$, and $z_d = \sum_i I(d_i = d, Z_i = 1)$, which represent the number of patients, patients experiencing DLT, and patients with efficacy response at dose d , separately. The factors in the four lines of (10) correspond to the likelihood function for the PK data and prior (the first line), efficacy response

data (the second line), toxicity response data (the third line), and prior for the dose-level parameters (the last line). Here, $g(\boldsymbol{\theta})$ denotes the prior distribution of $\boldsymbol{\theta}$, which will be elaborated in Section 4.

We use Markov chain Monte Carlo (MCMC) simulation to generate samples from the posterior distributions of the unknown parameters, with which statistical inference is conducted. The computation is implemented using R/JAGS.

2.5 Design Algorithm

Due to the model-based nature of PEDOOP, we follow the principle of the CRM design (O’Quigley et al., 1990). Specifically, PEDOOP allocates the first cohort of patients at the starting dose and continuously allocates subsequent cohorts to a dose that is deemed more beneficial to patients. Similar to the CRM design, let \hat{p}_d denotes the posterior mean of the toxicity probability of dose d given the current trial data \mathcal{D}_I . PEDOOP finds the dose d' for the next cohort given by

$$d' = \underset{d}{\operatorname{argmin}} |\hat{p}_d - p_T|.$$

However, if there is no DLT at the current dose and doses below the current dose, the next cohort is always treated at the dose one level above the current dose to speed up exploration. That is, $d' = d + 1$ if $\sum_i^d y_i = 0$, where d represents the current dose in the dose escalation. Furthermore, for safety, if $d^* = \underset{d}{\operatorname{argmin}} |\hat{p}_d - p_T|$, $d^* > d + 1$, and $n_{d^*-1} = 0$, then $d' = d + 1$. This is essentially no-skip in dose escalation, a common practice by the CRM design.

During the trial, a safety rule is added to avoid overdosing or terminate the trial if there are no safety doses. If dose d satisfies

$$\Pr(p_d > \pi_S \mid \mathcal{D}_I) < s^*,$$

then dose d is considered safe. Here, π_S and s^* are two prespecified parameters, and we can easily let $\pi_S = p_T$ and $s^* = 0.95$.

2.6 Graduation Rule

At the end of phase I, if a dose exhibits promising efficacy and low toxicity, it will graduate to phase II. We follow the SEARS design (Pan et al., 2014) and implement the following graduation rule: if dose d meets the two criteria in (11), it will graduate to the next phase and be compared in a randomized fashion.

$$\Pr(p_d < \pi_T \mid \mathcal{D}_I) > p^* \text{ and } \Pr(q_d > \pi_E \mid \mathcal{D}_I) > q^*, \quad (11)$$

where p_d and q_d denote the toxicity and efficacy probabilities of dose d , respectively. π_T , π_E , p^* and q^* are four physician-specified values. For example, π_T can be set to the target toxicity probability in phase I and π_E can be the

historical response rate of the standard treatment. If multiple doses satisfy the rules in (11), all of them are allowed to graduate to phase II depending on the resources. And if no dose satisfies the rules in (11), the trial stops.

3 Phase II Design

3.1 Utility

Assume doses $\{r \mid r = 1, \dots, R\}$ graduate from the phase I as per the graduation rule (11), which will be regarded as separate arms in phase II. Besides that, we assume that a control arm is included which could be the standard of care. Let $r = 0$ denote the control arm. The patient population in phase II is now restricted to a specific indication and enrolled patients are adaptively randomized to arms $\{r \mid r = 1, \dots, R\}$ and the control arm. We use a joint efficacy and toxicity outcome as the primary endpoint for the phase II trial. There are four possible bivariate binary outcomes for a patient, (No toxicity, No efficacy), (No toxicity, Efficacy), (Toxicity, No efficacy), and (Toxicity, Efficacy). We use a utility function to numerically score the four outcomes in the table below. The four utility values $\{s_1, s_2, s_3, s_4\}$ are used to describe the relative benefits of the treatment to a patient. We assume each $s_i \in [0, 1]$ without loss of generality. Apparently, s_1 should be the largest since it is associated with the best outcome (No toxicity, Efficacy) for a patient. We set $s_1 = 1$. Conversely, we let $s_4 = 0$. The other two values, s_2 and s_3 , are between 0 and 1 and are elicited from clinicians. Their values are contingent upon the specific circumstances and conditions encountered in real clinical trials. Specifically, for very aggressive cancers, s_2 could be larger than s_3 to reflect the desire for efficacy, while for less aggressive cancers, one may prefer a smaller s_2 than s_3 . In the proposed design, s_2 and s_3 are set to 0.6 and 0.4 temporarily.

Table 1: Utility of the joint efficacy toxicity outcomes. Each $0 \leq s_i \leq 1$ value represents the relative benefit of the outcome for a patient.

Efficacy \ Toxicity	No	Yes
	No	Yes
Yes	s_1	s_2
No	s_3	s_4

Let p_{r1} , p_{r2} , p_{r3} , and p_{r4} denote the probabilities of (No toxicity, Efficacy), (Toxicity, Efficacy), (No toxicity, No efficacy), and (Toxicity, No efficacy) for arm r , respectively. Note that $(p_{r1} + p_{r2})$ also represents the toxicity probability and $(p_{r2} + p_{r4})$ the efficacy probability. Given the probabilities $(p_{r1}, p_{r2}, p_{r3}, p_{r4})$ and the utilities (s_1, s_2, s_3, s_4) ,

we can calculate the expected utility of arm r by

$$u_r = \sum_{i=1}^4 s_i \times p_{ri}.$$

3.2 Patient Allocation

Let $(y_{r1}, y_{r2}, y_{r3}, y_{r4})$ denote the numbers of patients at dose d having outcomes (No toxicity, Efficacy), (Toxicity, Efficacy), (No toxicity, No efficacy), (Toxicity, No efficacy), respectively. Then the total utility of patients at arm r can be calculated by $S_r = \sum_{i=1}^4 s_i \times y_{ri}$. And S_r can be interpreted as the number of “events” observed among n_d patients treated at arm r given the event probability u_r . Following [Yuan et al. \(2007\)](#) and [Lin et al. \(2020\)](#), given $\{s_i; i = 1, \dots, 4\}$, we model the “quasi-binomial” data (S_r, n_r) with a quasi-binomial likelihood of the observe data (S_r, n_r) is

$$L((S_r, n_r) | u_r) \propto u_r^{S_r} (1 - u_r)^{n_r - S_r}$$

Under the Bayesian framework, we assign u_r a Beta prior, i.e. $u_r \sim \text{Beta}(\alpha, \beta)$, where α and β are the prespecified hyperparameters. By default, we set $\alpha = \beta = 1$, i.e., a weakly informative prior distribution for u_r . The posterior distribution of u_r arises as

$$u_r | (S_r, n_r) \sim \text{Beta}(\alpha + S_r, \beta + n_r - S_r).$$

Note that one could easily incorporate efficacy and toxicity data from phase I into the modeling. Denote the corresponding phase I quasi-binomial data as (S_{r1}, n_{r1}) . Then the posterior distribution of u_r is $\text{Beta}(\alpha + S_r + S_{r1}, \beta + n_r + n_{r1} - S_r - S_{r1})$.

Using the posterior distributions, we consider Bayesian adaptive randomization (BAR) procedures to continuously update the randomization probability for arm r . For example, a popular BAR approach randomizes patients to dose arm r with a probability proportional to the posterior probability that the efficacy probability of arm r , q_r , is larger than a prespecified threshold π_E given the observed data, i.e., $\Pr(q_r > \pi_E | \mathcal{D}_{\text{II}})$. Here, \mathcal{D}_{II} represents the observed data in phase II, and $\mathcal{D}_{\text{II}} = \{(y_{r1}, y_{r2}, y_{r3}, y_{r4}, n_r), r = 0, 1, \dots, R\}$. However, [Huang et al. \(2007\)](#) pointed out this approach does not reflect the relative desirability of each arm. Instead, they propose to randomize patients based on $\Pr(q_r > \max\{q_{r'}; r' \neq r\} | \mathcal{D}_{\text{II}})$ which can result in more patients treated in arms with relatively high efficacy rates.

We apply a BAR scheme similar to [Huang et al. \(2007\)](#). To take advantage of the quasi binomial utility, we replace the efficacy probability in their formula with the utility above. Thus, patients are randomized to arm r with a probability proportional to

$$\xi_r \equiv \Pr(u_r > \max\{u_{r'}; r' \neq r\} | \mathcal{D}_{\text{II}}) \quad (12)$$

3.3 Trial Design

We propose to update the randomization probabilities ξ_r after a cohort of n patients' outcomes are obtained, and the trial continues until the maximum sample size N is reached. The phase II part of the proposed PEDOOP design is as follows.

1. **Run in:** The first n patients as a cohort are randomized equally to the $(R + 1)$ arms.
2. Update the randomization probabilities ξ_r 's in (12).
3. The next cohort of n patients are randomized to arms $\{0, 1, \dots, R\}$ with ξ_r .
4. Repeat steps 2 and 3 until the maximum sample size N of phase II is reached.
5. Upon conclusion of the trial, recommend the arm with the highest posterior probability (12) to be further studied. If the control arm has the highest utility, no arm is recommended.

In practice, efficacy outcomes are usually observed much later than toxicity outcomes. In order to apply the above algorithm one should wait until the efficacy outcomes from the previous cohort are observed before updating the randomization probabilities, which would likely increase the duration of the trial depending on how fast patient accrual is. On the other hand, the proposed adaptive randomization can potentially increase the chance a patient is assigned to a more effective and safer arm. For a practical trial, the cohort size should be selected based on the observation time of efficacy and toxicity outcomes, enrollment speed, the number of arms in the trial, among other criteria. One may find a proper cohort size n by balancing the tradeoff among these criteria.

BAR procedures often employ practical steps to avoid undesirable performance. See [Thall and Wathen \(2007\)](#) and more recently [Robertson et al. \(2023\)](#) for comprehensive reviews. Since the methodology of BAR is not the focus of this work, we do not go into detail on how BAR could be improved with recommendations in the cited works. In practice, we recommend applying the additional rules in the two papers in order to further improve the performance of the BAR algorithm above.

3.4 Arm Selection

At the end of phase II, several doses among $\{r \mid r = 1, \dots, R\}$ will be recommended to the next phase. The SEARS design ([Pan et al., 2014](#)) implemented the following selection rule: if arm r meets the two criteria (13), it will be recommended to the next phase. Let

$$C = \{r : \Pr(p_r < \pi_T \mid \mathcal{D}_{\text{II}}) > p^{**} \text{ and } \Pr(q_r > \pi_E \mid \mathcal{D}_{\text{II}}) > q^{**}\}, \quad (13)$$

where p_r and q_r denote the toxicity and efficacy probabilities of arm r . And the posterior distributions of p_r and q_r are both based on the beta prior, $Beta(1, 1)$. p^{**} and q^{**} are two physician-specified values. Criteria (13) will potentially lead to selecting more than one dose, and we call these “admissible doses”.

We also propose to select the dose with the highest utility based on posterior probability (12) among those meeting the criteria (13). That is, the dose r^* is selected where

$$r^* = \operatorname{argmax}_{r \in C} \xi_r = \operatorname{argmax}_{r \in C} \Pr(u_r > \max\{u_{r'}; r' \neq r\} \mid \mathcal{D}_{\Pi}).$$

Dose r^* is the estimated OBD.

4 Simulation Study

4.1 Prior Distribution

In our simulation studies, we adopt the following prior distributions for model parameters.

$$\begin{aligned} \alpha_V - 1 &\sim \text{Gamma}(4, 1), \quad \lambda_V \sim \text{Gamma}(1, 1), \\ \alpha_k - 1 &\sim \text{Gamma}(3, 1), \quad \lambda_k \sim \text{Gamma}(1, 1), \\ \sigma &\sim \text{Gamma}(3, 3), \\ \beta_0 &\sim N(-3, 10^2), \quad \beta_1 \sim \text{LogN}(-1, 2), \\ E_{\max} &\sim \text{LogN}(-1, 0.5), \quad ED_{50} \sim \text{Gamma}(20, 0.5), \quad \text{and} \quad \phi \sim \text{Cat}(4, \mathbf{p}), \end{aligned} \tag{14}$$

where $\phi \in \{2, 3, 4, 5\}$ and $\mathbf{p} = (0.25, 0.25, 0.25, 0.25)$. Here, the shape parameters α_V and α_k follow $1 + \text{Gamma}(4, 1)$ and $1 + \text{Gamma}(3, 1)$ distributions. This assumption ensures that $\alpha_V > 1$ and $\alpha_k > 1$, which are necessary conditions for a closed-form solution of dose-level parameters, such as the dose-level AUC in (5).

The hyperparameters in (14) are determined so that the corresponding priors of p_d and q_d are vague distributions. Specifically, with the priors in (14), the corresponding prior distribution of p_d can be numerically determined according to equations (5) and (6), and q_d according to (9). We plot the corresponding prior densities of p_d and q_d , $d = 1, \dots, D$ in Figure 2. The plots show that the priors of p_d ’s are of small density values in most of the parameter space.

4.2 Simulation 1

4.2.1 Simulation Setup

To assess the impact of integration of PK data like the time-course drug concentration, we perform 1,000 simulated trials to compare the proposed PEDDOOP design and a simpler model, called “DOOP”, meaning PEDDOOP without

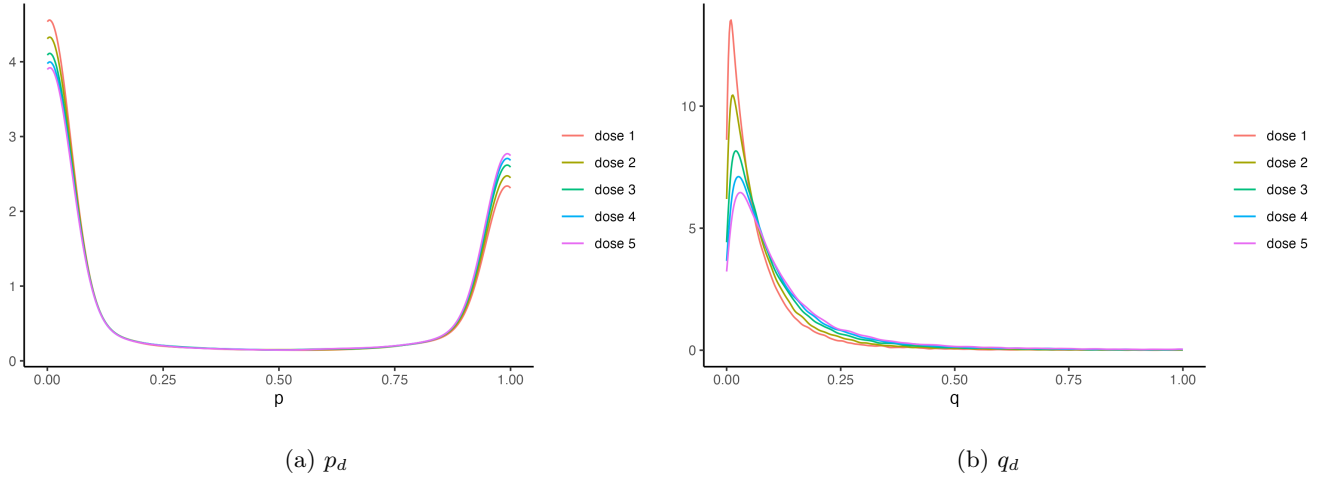


Figure 2: Density of prior distributions of p_d and q_d , $d = 1, \dots, D$, given hyperparameters in (14).

P (PK) or E (enabled). Specifically, DOOP adopts the same designs as PEDOOP described in Sections 2.5, 2.6, and 3 but does not incorporate PK data. Instead, DOOP simply uses a logit regression model (15) on toxicity and an Emax model (16) on efficacy without integrating PK data, i.e.,

$$\text{logit}(\tilde{p}_d) = \tilde{\beta}_0 + \tilde{\beta}_1 \times \log(d). \quad (15)$$

For DOOP, we adopt similar priors as in PEDOOP.

$$\text{logit}(\tilde{q}_d) = 1 - \exp(-\tilde{\eta}(d)), \quad \text{where} \quad \tilde{\eta}(d) = \frac{\tilde{E}_{\max} \times d^{\tilde{\gamma}}}{\widetilde{ED}_{50} + d^{\tilde{\gamma}}}. \quad (16)$$

$$\begin{aligned} \tilde{\beta}_0 &\sim N(-3, 10^2), \quad \tilde{\beta}_1 \sim \text{LogN}(-1, 2), \\ \tilde{E}_{\max} &\sim \text{LogN}(-1, 0.5), \quad \widetilde{ED}_{50} \sim \text{Gamma}(10, 0.1), \quad \text{and} \quad \tilde{\gamma} \sim \text{Gamma}(0.1, 0.1). \end{aligned} \quad (17)$$

The joint posterior distribution of $\tilde{\boldsymbol{\theta}} = \{\tilde{\beta}_0, \tilde{\beta}_1, \tilde{E}_{\max}, \widetilde{ED}_{50}, \tilde{\gamma}\}$ can be written as

$$\pi(\tilde{\boldsymbol{\theta}} \mid \mathcal{D}_I) \propto \left\{ \prod_d \tilde{p}_d^{y_d} (1 - \tilde{p}_d)^{n_d - y_d} \right\} \times \left\{ \prod_d \tilde{q}_d^{z_d} (1 - \tilde{q}_d)^{n_d - z_d} \right\} \times g(\tilde{\boldsymbol{\theta}}),$$

where $g(\tilde{\boldsymbol{\theta}})$ denotes the prior distribution of $\tilde{\boldsymbol{\theta}}$.

For simplicity, in this section, we only compare the phase I simulation results of PEDOOP and DOOP since the phase II portion of both designs are identical. The target toxicity rate is set to $p_T = 0.3$. We assume that there are five dose levels, i.e., $d \in (15, 30, 60, 90, 120)$, and drug concentration are measured for each patient six times, at 1, 3, 5, 7, 12, and 24 hours after administration. A maximum of 30 patients with three patients as a cohort is to be enrolled in phase I. For both designs, $\pi_T = 0.3$, $p^* = 0.6$, $q^* = 0.6$, and $\pi_E = 0.2$ in the graduation rule (11).

Here we generate the patient-specific elimination rate and volume of distribution k and V for 30 individuals randomly through gamma distributions, and the generated V and k values are subsequently used to generate drug concentration data X using a normal distribution. For example, for patient i , the corresponding values are generated via

$$V_i \sim \text{Gamma}(4, 1), \quad k_i \sim \text{Gamma}(3, 1), \quad \log(X_{ij}) \mid V_i, k_i \sim N\left(\log\left(\frac{d_i}{V_i}\right) - k_i t_j, 1\right), \quad (18)$$

where $d_i \in \{7, 15, 30, 60, 120, 150\}$ and $t_j \in \{1, 3, 5, 7, 12, 24\}$. We set $E_{\max} = 1$, $ED_{50} = 100$, and $\phi = 2$ for all the scenarios. Given the true parameter values, the cumulative effect of the test drug is generated via (8), which is substituted into (9) to generate the efficacy probabilities for the five dose levels. This leads to true efficacy probabilities (0.12, 0.18, 0.27, 0.33, 0.37) for all the scenarios. To generate true toxicity probabilities, we first compute the dose level AUC via (5) and then assign different values of (β_0, β_1) scenarios 1 through 4 in (6) as $\{(-2.5, 1), (-3, 0.95), (-4.5, 1.35), (-2.5, 0.5)\}$. This leads to the true toxicity probabilities in Table 2.

Figure 3 presents the density plots of the logarithm of AUC for the five doses in a simulated trial. The logarithm AUC is numerically calculated according to (5). It shows that the posterior distribution is able to shrink the prior towards the truth.

In this simulation study, we set up a total of four distinct scenarios. To create these scenarios, we held the true values of θ constant, thereby determining the toxicity and efficacy probabilities for each one.

4.2.2 Simulation Results

The operating characteristics of the PEDOOP and DOOP models are summarized in Table 2. We compare PEDOOP and DOOP based on two key factors, patient allocation and dose selection by the models. We begin by presenting the selection frequency of doses at the end of phase I according to the graduation rule (11). We refer to these doses the ‘‘admissible doses’’. It’s worth noting that the graduation rule may lead to the selection of multiple doses at the end of phase I. This feature enables phase II to employ adaptive randomization for a further exploration of these doses. Also, we present the selection frequency of doses based on the graduation rule (11) and the highest posterior probability (12), where no more than one dose is recommended to phase II in each simulated trial. The dose with the highest posterior probability among the admissible doses is considered the OBD.

In general, PEDOOP and DOOP allocate comparable numbers of patients to the OBDs in the four scenarios. In view of OBD selection frequency, PEDOOP is more desirable than DOOP.

In scenario 1, there are no desirable doses since the first two doses of the tested drug have lower efficacy probabilities than π_E , while the last three have higher toxicity probabilities than π_T . PEDOOP exhibits a lower frequency of selecting either dose than DOOP. In scenarios 2, 3 and 4, , doses 3, 4, and 5 are the true OBD respectively.

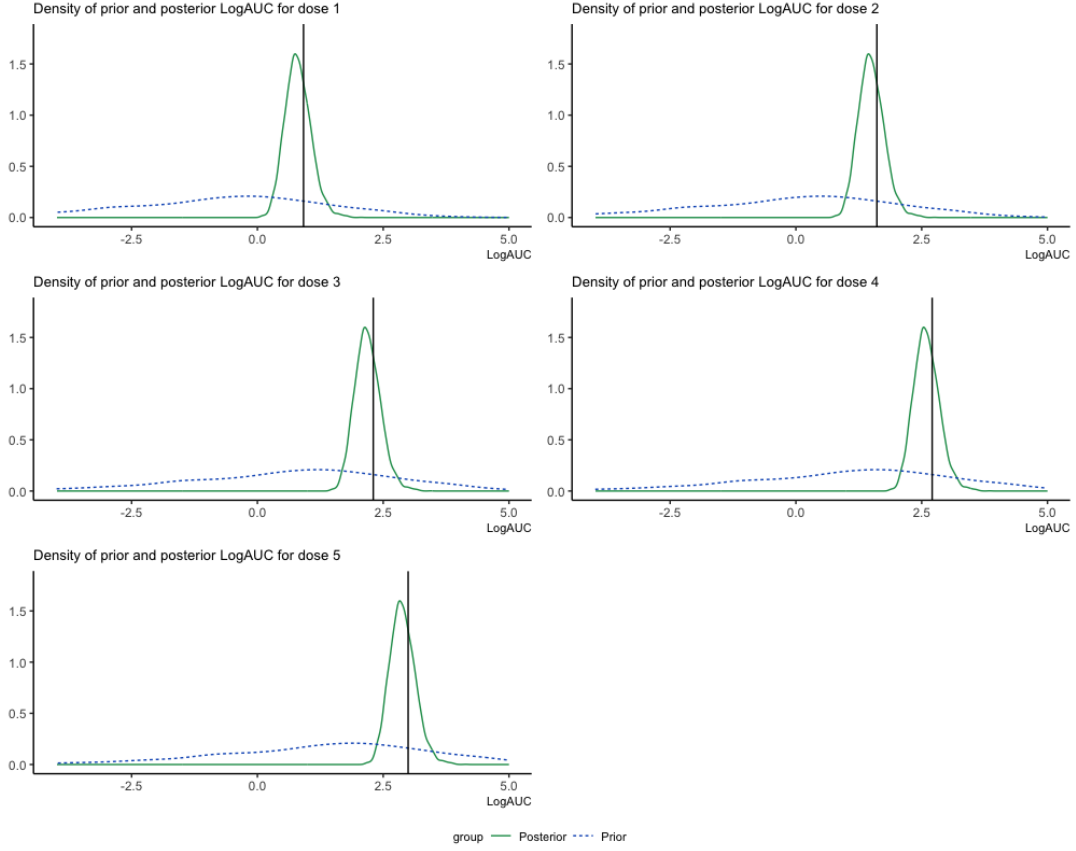


Figure 3: Densities of the prior and posterior distributions of the logarithm of AUC for five doses in a simulated trial. The green solid line represents the posterior distribution, while the blue dashed line represents the prior distribution. And the vertical line denotes the logarithm of the true AUC.

PEDOOP presents a higher frequency of selecting the true OBD in all three scenarios.

We also investigate the estimation of ϕ , and present the posterior estimates of ϕ in Table A.1. Overall, the estimates are reasonable, close to its true value of 2.

Table 2: Phase I simulation results of Simulation 1. Here, the bold font indicates the true OBD in each scenario, which has a toxicity rate closest to $p_T = 0.3$ and an efficacy rate larger than $\pi_E = 0.2$. And “Admissible Doses” and “OBD” represent the selection frequency as admissible doses and OBD in percentage, respectively.

		Dose	1	2	3	4	5
		True Eff. Prob.	0.12	0.18	0.27	0.33	0.37
Sc 1	PEDOOP	True Tox. Prob.	0.17	0.29	0.45	0.55	0.62
		Utility	0.404	0.392	0.382	0.378	0.374
		# of Patients	10.494	11.163	5.79	1.587	0.627
		Admissible Doses	1.5	6.6	3.5	0.1	0.2
		OBD	1	5.6	2.8	0	0.1
	DOOP	# of Patients	10.032	11.343	6.057	1.608	0.573
		Admissible Doses	22.5	18.3	4.2	0.5	0.4
		OBD	14.3	9.8	2.1	0.2	0.1
Sc 2	PEDOOP	True Tox. Prob.	0.11	0.19	0.31	0.39	0.46
		Utility	0.428	0.432	0.438	0.442	0.438
		# of Patients	5.64	7.728	8.217	4.725	3.588
		Admissible Doses	2.8	14.5	24.4	12.5	5.2
		OBD	1	8.6	16.4	6.6	2.4
	DOOP	# of Patients	5.523	7.728	8.178	4.512	4.008
		Admissible Doses	36.6	36.9	24.2	11.5	3.7
		OBD	13.7	15.8	12.3	6.4	1.4
Sc 3	PEDOOP	True Tox. Prob.	0.04	0.09	0.2	0.3	0.39
		Utility	0.456	0.472	0.482	0.478	0.466
		# of Patients	3.492	3.99	6.78	7.017	8.721
		Admissible Doses	2.8	21.5	47.4	35.7	18.5
		OBD	0.7	9	28.1	17.7	7.8
	DOOP	# of Patients	3.606	4.062	6.786	6.45	9.069
		Admissible Doses	39.6	45.6	51.8	33.2	13
		OBD	10.7	17.3	23.6	14.4	5.8
Sc 4	PEDOOP	True Tox. Prob.	0.11	0.16	0.21	0.24	0.27
		Utility	0.428	0.444	0.478	0.502	0.514
		# of Patients	5.388	5.325	5.34	4.077	9.792
		Admissible Doses	2	15.3	43.1	47	39.3
		OBD	0.4	6	18.8	22.3	16
	DOOP	# of Patients	5.244	4.971	5.367	4.227	10.116
		Admissible Doses	33.4	38	44.5	41.5	28.7
		OBD	8.6	15	17.2	18	11.6

4.2.3 Sensitivity Analysis

We conduct a small sensitivity analysis to check the robustness of model misspecification, especially on the PK modeling. We modify the generative model in (18) and assume a new model given by

$$V_i \sim \text{Gamma}(4, 1), \quad k_i \sim 1 + \text{Gamma}(3, 1), \quad \log(X_{ij}) \mid V_i, k_i \sim N\left(\frac{d_i}{V_i} - k_i^{e_i} t_j, 1\right), \quad (19)$$

where $e_i \sim \text{Beta}(1, d_i)$. Since $k_i > 1$, and e_i decreases with d_i in probability, (19) allows the patient-specific elimination rate $k_i^{e_i}$ to be lower for a higher dose. The generative model (19) is now different from the true model (18) for PEDOOP. We re-run simulations with the new generative model of X_{ij} and summarize the new simulation results in Table 3. We call the new approach “PEDOOP–w” with “w” standing for the wrong fitting model. It can be seen that the performance of PEDOOP–w drops in scenario 1 selecting the non-promising doses 1 and 2 with much higher frequencies. For other scenarios, PEDOOP–w performs similarly to PEDOOP. These results suggest that when the PK-model is misspecified, the performance of PEDOOP is somewhat robust (as seen in Scenarios 2-4). However, in Scenario 1 when all doses are either too toxic or not effective, the model misspecification has more impact and reduced the performance of the design.

4.3 Simulation 2

4.3.1 Simulation Setup

We perform 1,000 simulation studies to compare the proposed PEDOOP design and the SEARS design (Pan et al., 2014). In phase I, similarly we assume that there are seven dose levels, (15, 30, 60, 90, 120), and drug concentration are measured for each patient six times, at 1, 3, 5, 7, 12, and 24 hours after administration. A maximum of 30 patients with three patients a cohort is to be enrolled in phase I. The maximum sample size of phase II is set to 150 with 10 patients a cohort. This means that the BAR randomization probability is updated every 10 patients in phase II. Similarly, the maximum sample size of phase I for the SEARS design is set to 30, and the maximum sample size of the both phases under the SEARS design is set to 180. Besides, the SEARS design considered a maximum sample size of 36 patients for each dose and the control arm. For both designs, $\pi_T = 0.2$, $p^* = 0.6$, $q^* = 0.6$, and $\pi_E = 0.2$ in the graduation rule (11) at the end of phase I, and $p^{**} = 0.7$ and $q^{**} = 0.9$ in the selection criteria (13) at the end of phase II.

In phase I, we generate the patient-specific elimination rate, k , volume of distribution V , and drug concentration data X for 30 individuals randomly via

$$V_i \sim \text{Gamma}(10, 1), \quad k_i \sim \text{Gamma}(9, 1.5), \quad \log(X_{ij}) \mid V_i, k_i \sim N\left(\log\left(\frac{d_i}{V_i}\right) - k_i t_j, 4^2\right), \quad (20)$$

Table 3: Sensitivity analysis comparing the proposed PEDOOP design with the same design but using a wrong model (PEDOOP-w) for generating the simulated data. The bold font indicates the true OBD in each scenario, which has a toxicity rate closest to $p_T = 0.3$ and an efficacy rate larger than $\pi_E = 0.2$. PEDOOP represents the simulation results given the generative model in (18), while “PEDOOP-w” represents those given the “wrong” generative model in (19). For simplicity, we only present frequencies of selecting the OBD and omit the ones for Admissible dose.

		Dose	1	2	3	4	5
		True Eff. Prob.	0.12	0.18	0.27	0.33	0.37
Sc 1		True Tox. Prob.	0.17	0.29	0.45	0.55	0.62
		Utility	0.404	0.392	0.382	0.378	0.374
	PEDOOP	# of Patients	10.494	11.163	5.79	1.587	0.627
		OBD	1	5.6	2.8	0	0.1
	PEDOOP-w	# of Patients	10.719	10.167	6.093	1.731	0.9
		OBD	11.9	8	2.2	0.3	0.1
Sc 2		True Tox. Prob.	0.11	0.19	0.31	0.39	0.46
		Utility	0.428	0.432	0.438	0.442	0.438
	PEDOOP	# of Patients	5.64	7.728	8.217	4.725	3.588
		OBD	1	8.6	16.4	6.6	2.4
	PEDOOP-w	# of Patients	5.745	6.894	7.914	4.296	5.049
		OBD	5.8	12.8	16.2	6.9	2.5
Sc 3		True Tox. Prob.	0.04	0.09	0.2	0.3	0.39
		Utility	0.456	0.472	0.482	0.478	0.466
	PEDOOP	# of Patients	3.492	3.99	6.78	7.017	8.721
		OBD	0.7	9	28.1	17.7	7.8
	PEDOOP-w	# of Patients	3.579	4.011	6.594	5.628	10.188
		OBD	2	8.4	29.2	18	8.8
Sc 4		True Tox. Prob.	0.11	0.16	0.21	0.24	0.27
		Utility	0.428	0.444	0.478	0.502	0.514
	PEDOOP	# of Patients	5.388	5.325	5.34	4.077	9.792
		OBD	0.4	6	18.8	22.3	16
	PEDOOP-w	# of Patients	5.133	4.608	4.959	3.747	11.529
		OBD	2.5	5.6	18.1	26.5	18.9

where $d_i \in \{15, 30, 60, 90, 120\}$ and $t_j \in \{1, 3, 5, 7, 12, 24\}$.

We set up a total of 12 scenarios in the simulation study. All the scenarios have the same control arm with a toxicity probability of 0.17 and an efficacy probability of 0.2. Following [Pan et al. \(2014\)](#), we only consider two types of toxicity profile. That is, scenarios 1 to 6 are with toxicity probabilities (0.03, 0.06, 0.17, 0.3, 0.5), which means that the third dose of the tested drug has equal toxicity as the control arm, and the fourth one is more toxic than the control arm. Scenarios 7 to 12 are with toxicity probabilities (0.03, 0.06, 0.09, 0.12, 0.15), where any dose is with less toxic than the control arm.

In scenarios 1 and 7, the efficacy probability stays flat regardless of the dose. Therefore, the first dose is the optimal one in the two scenarios. The efficacy probability in scenarios 2 and 8 increases with dose, while in contrast efficacy probability decreases with dose in scenarios 3 and 9. Scenarios 4 and 10 have a N-shape efficacy probability and scenarios 5 and 11 have a U-shape efficacy probability, although the two types are not common. Efficacy probability in scenarios 6 and 12 reaches a plateau and stays flat after a certain dose level. Specific information can be found in [Tables 4 and 5](#).

4.3.2 Simulation Results

The operating characteristics of the PEDOOP and SEARS designs are summarized in [Tables 4 and 5](#). In this simulation study, “Admissible Doses” is presented to indicate the selection frequency of each dose at the end of phase II according to the criteria [\(13\)](#). This rule may lead to the selection of multiple doses. Also, we present the “OBD” is based on the criteria [\(13\)](#) and the highest posterior probability [\(12\)](#), where a maximum of one dose is selected.

In scenarios 1 and 7, there are no desirable doses since all doses of the tested drug have the same efficacy probability as the control arm. The PEDOOP design stop trials with fewer enrolled patients, allocating on average 9.877 and 12.228 patients to doses 2 and 3 in scenario 1, respectively, compared with 18.483 and 19.428 patients by SEARS. PEDOOP also selects doses with less frequencies, which is as expected since no doses should be selected under the two scenarios.

In scenarios 2 and 6, the optimal dose for both scenarios is dose 3. Dose 2 is the second optimal with a similar utility. PEDOOP and SEARS select doses 2 and 3 with similar frequencies, but SEARS tends to allocate more patients to toxic doses, e.g., doses 4 and 5, than PEDOOP.

In scenarios 8 and 12, none of the doses are toxic as their toxicity probabilities are all below p_T . Therefore, the optimal dose is the one with the highest efficacy probability. In scenario 8, the efficacy probability increases with the dose level, and dose 5 is optimal. In scenario 12, the efficacy probability reaches a plateau after dose 3, making it the optimal dose. PEDOOP and SEARS allocate similar numbers of patients to the doses while PEDOOP selects

the optimal dose with a lower proportion than SEARS.

In scenarios 3, 5, 9, and 11, the optimal dose is dose 1 for all of them based on the truth. In terms of patient allocation, PEDOOP perform similar to SEARS. However, PEDOOP selects the optimal dose with less frequencies. This is potentially due to the fact that efficacy does not increase with dose in these scenarios, which violates the monotonic efficacy assumption in (9).

In scenarios 4 and 10, efficacy probabilities of doses display an “n” shape. Dose 3 has the highest efficacy, and it is the optimal dose. In terms of patient allocation, PEDOOP is safer than SEARS in scenario 4 as it allocates more patients to doses 1 and 2 and fewer patients to doses 3 to 5 than SEARS. In scenario 10, all doses of the tested drug are safe, and PEDOOP tends to allocate more patients to dose 5. Both designs select the optimal dose in a similar fashion in both scenarios.

In most scenarios, “OBD” of the optimal dose did not decrease significantly compared to “Admissible Doses”. However, in scenarios 3, 11, and 12, “OBD” of the optimal dose dropped considerably. This is primarily because other doses also have high utilities, similar to the optimal one. For example, in scenario 12, dose 3 has the highest utility of 0.664, while doses 4 and 5 are with 0.652 and 0.64. Therefore, it is difficult to differentiate between these doses.

Table 4: Simulation results of scenarios 1 to 6 in Simulation 2.

		Dose	1	2	3	4	5	Control
		True Tox. Prob.	0.03	0.06	0.17	0.3	0.5	0.17
		AUC	0.31	0.62	1.25	1.88	2.5	
Sc 1	PEDOOP	True Eff. Prob.	0.2	0.2	0.2	0.2	0.2	0.2
		Utility	0.508	0.496	0.452	0.4	0.32	0.452
		# of Patients	5.519	9.877	12.228	6.049	2.818	3.558
		Admissible Doses	0.3	1.3	1	0	0	
		OBD	0.3	1.2	1	0	0	
	SEARS	# of Patients	16.968	18.483	19.428	11.652	2.982	14.304
		Admissible Doses	7.3	6.5	3.2	0.2	0	
Sc 2	PEDOOP	True Eff. Prob.	0.2	0.3	0.5	0.7	0.8	0.2
		Utility	0.508	0.556	0.632	0.7	0.68	0.452
		# of Patients	17.826	25.598	22.326	7.518	3.116	14.622
		Admissible Doses	7.4	37.9	27.9	0.8	0	
		OBD	4	29.5	25	0.8	0	
	SEARS	# of Patients	12.216	17.349	25.176	16.164	3.561	10.293
		Admissible Doses	10.4	35.4	34.7	1.8	0	
Sc 3	PEDOOP	True Eff. Prob.	0.8	0.7	0.5	0.3	0.2	0.2
		Utility	0.868	0.796	0.632	0.46	0.32	0.452
		# of Patients	32.189	25.086	14.988	6.322	2.838	5.325
		Admissible Doses	90.9	81.3	25.2	0.2	0	
		OBD	76.1	19.5	0.6	0	0	
	SEARS	# of Patients	30.039	23.022	15.153	8.535	2.922	5.754
		Admissible Doses	94.9	85.1	28.7	1.9	0	
Sc 4	PEDOOP	True Eff. Prob.	0.2	0.4	0.8	0.4	0.2	0.2
		Utility	0.508	0.616	0.812	0.52	0.32	0.452
		# of Patients	14.372	23.361	24.709	6.432	2.839	11.146
		Admissible Doses	6.6	57.7	28.5	0.9	0	
		OBD	2.3	41.6	28.5	0.1	0	
	SEARS	# of Patients	9.435	15.165	30.399	8.913	2.646	7.032
		Admissible Doses	8.2	52.6	37.9	3.4	0.1	
Sc 5	PEDOOP	True Eff. Prob.	0.8	0.4	0.2	0.4	0.8	0.2
		Utility	0.868	0.616	0.452	0.52	0.68	0.452
		# of Patients	31.85	15.688	14.06	6.436	2.848	6.35
		Admissible Doses	75.8	46.8	2.9	0.9	0	
		OBD	75.8	8.2	0	0	0	
	SEARS	# of Patients	31.851	12.351	11.739	9.522	3.456	6.318
		Admissible Doses	88.5	44.4	4.5	2.1	0	
Sc 6	PEDOOP	True Eff. Prob.	0.2	0.4	0.5	0.5	0.5	0.2
		Utility	0.508	0.616	0.632	0.58	0.5	0.452
		# of Patients	16.195	29.79	21.727	6.878	3.041	12.047
		Admissible Doses	7.4	69.5	29.9	0.9	0	
		OBD	2.7	55.7	21	0.6	0	
	SEARS	# of Patients	12.162	21.708	26.586	13.68	3.519	10.491
		Admissible Doses	8.6	66.8	37	1.8	0	

Table 5: Simulation results of scenarios 7 to 12 in Simulation 2.

		Dose	1	2	3	4	5	Control
		True Tox. Prob.	0.03	0.06	0.09	0.12	0.15	0.17
		AUC	0.31	0.62	1.25	1.88	2.5	
Sc 7	PEDOOP	True Eff. Prob.	0.2	0.2	0.2	0.2	0.2	0.2
		Utility	0.508	0.496	0.484	0.472	0.46	0.452
		# of Patients	4.713	6.416	7.803	7.45	15.088	4.426
		Admissible Doses	0.4	0.9	1.9	2.2	1.8	
		OBD	0.4	0.9	1.6	1.9	1.6	
	SEARS	# of Patients	16.86	16.668	17.475	18.054	17.916	15.189
		Admissible Doses	5.9	6.8	6.3	5.4	4.9	
Sc 8	PEDOOP	True Eff. Prob.	0.2	0.3	0.5	0.7	0.8	0.2
		Utility	0.508	0.556	0.664	0.772	0.82	0.452
		# of Patients	7.456	10.085	14.034	18.842	26.272	8.6
		Admissible Doses	4.5	18.4	40.1	45.1	42.7	
		OBD	1.1	6.3	13.4	27.1	37.8	
	SEARS	# of Patients	7.683	10.164	14.748	22.194	25.788	6.537
		Admissible Doses	7.9	21	54.9	58.2	43.9	
Sc 9	PEDOOP	True Eff. Prob.	0.8	0.7	0.5	0.3	0.2	0.2
		Utility	0.868	0.796	0.664	0.532	0.46	0.452
		# of Patients	26.843	20.797	13.631	8.349	13.704	6.392
		Admissible Doses	70.8	65.6	42.3	9.6	0.7	
		OBD	61	19.6	7.1	1.3	0.1	
	SEARS	# of Patients	27.81	20.925	12.942	9.867	9.483	6.048
		Admissible Doses	86.5	75.5	45.4	14.6	4.2	
Sc 10	PEDOOP	True Eff. Prob.	0.2	0.4	0.8	0.4	0.2	0.2
		Utility	0.508	0.616	0.844	0.592	0.46	0.452
		# of Patients	6.267	11.257	27.68	10.503	14.708	6.811
		Admissible Doses	3	31.9	60.9	21.5	1	
		OBD	0.1	7.5	60.6	5.4	0.4	
	SEARS	# of Patients	7.881	11.847	30.69	11.46	9.27	6.465
		Admissible Doses	7.8	42.5	77.2	27.2	3.9	
Sc 11	PEDOOP	True Eff. Prob.	0.8	0.4	0.2	0.4	0.8	0.2
		Utility	0.868	0.616	0.484	0.592	0.82	0.452
		# of Patients	31.639	9.546	6.451	7.257	24.252	5.948
		Admissible Doses	90	30.7	2.5	12.7	41.3	
		OBD	75.4	2	0	0.8	17.7	
	SEARS	# of Patients	25.194	9.927	9.18	10.95	23.583	5.706
		Admissible Doses	86.4	37.9	6.9	27.7	43.5	
Sc 12	PEDOOP	True Eff. Prob.	0.2	0.4	0.5	0.5	0.5	0.2
		Utility	0.508	0.616	0.664	0.652	0.64	0.452
		# of Patients	8.916	17.566	22.636	18.463	19.22	10.558
		Admissible Doses	4.5	46.7	55.1	41.6	23.8	
		OBD	0.6	18.3	34.6	24.7	13	
	SEARS	# of Patients	10.635	18.051	23.328	22.206	21.315	9.432
		Admissible Doses	11.3	58	70.8	56.2	39.6	

5 Discussion

Phase I trials typically collect data on toxicity, efficacy, PK, and PD of a new drug. However, most existing phase I dose-finding designs only focus on toxicity and efficacy outcomes, ignoring the PK and PD information. This may lead to inconsistency between the MTD identified by these designs and the optimal dose suggested by the PK and PD data. In this paper, we propose a statistical model that incorporates toxicity, efficacy, PK, and PD outcomes meanwhile to facilitate better dose selection in phase I trials, which is also the main contribution of this paper. A novel feature of the model is the use of dose-level AUC and PD, rather than patient-level ones, as covariates for toxicity and efficacy probabilities. Another contribution of this paper is the simulation of phase II trials to demonstrate the practicality and advantages of the proposed model.

In the proposed model, we assume that toxicity and efficacy increase monotonically with the dose level. However, in real trials, there may be various possible scenarios. The model may need to be adjusted according to the actual drug properties.

In phase II, we set a cohort size of 10 to match that in the SEARS design (Pan et al., 2014). In practical trials, the choice of the optimal cohort size should take into account the enrollment speed, followup time for efficacy and toxicity outcomes, trial duration, logistic cost and burden, and benefits from adjusting randomization probabilities. It is worth more consideration for future work.

The proposed PEDOOP design enrolls patients in cohorts in phase II. After patients in a cohort are randomized at doses graduated from phase I or the control arm, they are followed for a period of time for toxicity and efficacy outcomes. Then, the randomization probabilities are updated based on the posterior distribution of the proposed utilities of arms in Section 3.1, which are only based on toxicity and efficacy outcomes. We did not consider PK/PD in Phase II simply because they might not be available in time in practical situations as these measurements usually take time to produce in real life. We assume that the Phase II design would only use toxicity and efficacy outcomes for calculating patients allocation probabilities in the proposed BAR procedure, but at the end, a dose selection and go/no-go decision will be made based on all the data, including clinical and PK/PD data.

Finally, the proposed model is based on a first-order one-compartment model for the IV injection. This is a basic model in PK models. In future research, the proposed model can be extended to more situations. For example, the PK model we used leads to a linear relationship between AUC and dose which may not hold for certain therapeutics like monoclonal antibodies (mAbs) (Tabrizi et al., 2006). This is because binding of the drug to the target becomes a clearance mechanism, which may lead to potential alterations in clearance, particularly at lower doses. As the dose increases, the target-mediated clearance becomes saturated, and drug exposure may then become linear. Moreover, we introduce the concept of drug effect density (7) in the proposed model to link drug concentration with PD and

efficacy. This can also be realized by replacing the population-level drug concentration $c(t \mid d)$ with the area under the concentration-time curve $AUC(d)$. To improve the practical utility of our models, we may further elaborate on this adjustment and discuss how it can enhance precision in capturing drug-response relationships, as well as a more sophisticated Emax model, outlined in $r(d) = E_0 + \frac{E_{\max} \times (AUC(d))^\gamma}{ED_{50}^\gamma + (AUC(d))^\gamma}$.

Acknowledgement

We thank Michael J. Fossler for providing insightful comments.

References

- Abramowitz, M. and Stegun, I. A. (1968). *Handbook of mathematical functions with formulas, graphs, and mathematical tables*, volume 55. US Government printing office.
- Guo, W., Wang, S.-J., Yang, S., Lynn, H., and Ji, Y. (2017). A Bayesian interval dose-finding design addressing Ockham’s razor: mTPI-2. *Contemporary clinical trials*, 58:23–33.
- Huang, X., Biswas, S., Oki, Y., Issa, J.-P., and Berry, D. A. (2007). A parallel phase I/II clinical trial design for combination therapies. *Biometrics*, 63(2):429–436.
- Ji, Y., Liu, P., Li, Y., and Nebiyu Bekele, B. (2010). A modified toxicity probability interval method for dose-finding trials. *Clinical trials*, 7(6):653–663.
- Lin, R., Zhou, Y., Yan, F., Li, D., and Yuan, Y. (2020). BOIN12: Bayesian optimal interval phase I/II trial design for utility-based dose finding in immunotherapy and targeted therapies. *JCO precision oncology*, 4:1393–1402.
- Liu, M., Wang, S.-J., and Ji, Y. (2020). The i3+3 design for phase I clinical trials. *Journal of biopharmaceutical statistics*, 30(2):294–304.
- Liu, S. and Yuan, Y. (2015). Bayesian optimal interval designs for phase I clinical trials. *Journal of the Royal Statistical Society. Series C (Applied Statistics)*, 64(3):507–523.
- Meibohm, B. and Derendorf, H. (1997). Basic concepts of pharmacokinetic/pharmacodynamic (PK/PD) modelling. *International journal of clinical pharmacology and therapeutics*, 35(10):401–413.
- O’Quigley, J., Pepe, M., and Fisher, L. (1990). Continual reassessment method: a practical design for phase 1 clinical trials in cancer. *Biometrics*, pages 33–48.
- Pan, H., Xie, F., Liu, P., Xia, J., and Ji, Y. (2014). A phase I/II seamless dose escalation/expansion with adaptive randomization scheme (SEARS). *Clinical Trials*, 11(1):49–59.
- Patterson, S., Francis, S., Ireson, M., Webber, D., and Whitehead, J. (1999). A novel Bayesian decision procedure for early-phase dose-finding studies. *Journal of biopharmaceutical statistics*, 9(4):583–597.
- Piantadosi, S. and Liu, G. (1996). Improved designs for dose escalation studies using pharmacokinetic measurements. *Statistics in medicine*, 15(15):1605–1618.

- Robertson, D. S., Lee, K. M., López-Kolkovska, B. C., and Villar, S. S. (2023). Response-adaptive randomization in clinical trials: from myths to practical considerations. *Statistical science: a review journal of the Institute of Mathematical Statistics*, 38(2):185.
- Shargel, L., Andrew, B., and Wu-Pong, S. (1999). *Applied biopharmaceutics & pharmacokinetics*, volume 264. Appleton & Lange Stamford.
- Storer, B. E. (1989). Design and analysis of phase I clinical trials. *Biometrics*, pages 925–937.
- Su, X., Li, Y., Müller, P., Hsu, C.-W., Pan, H., and Do, K.-A. (2022). A semi-mechanistic dose-finding design in oncology using pharmacokinetic/pharmacodynamic modeling. *Pharmaceutical statistics*, 21(6):1149–1166.
- Tabrizi, M. A., Tseng, C.-M. L., and Roskos, L. K. (2006). Elimination mechanisms of therapeutic monoclonal antibodies. *Drug discovery today*, 11(1-2):81–88.
- Thall, P. F. and Wathen, J. K. (2007). Practical bayesian adaptive randomisation in clinical trials. *European Journal of Cancer*, 43(5):859–866.
- Ting, N. and Ting, N. (2006). *Dose finding in drug development*, volume 510. Springer.
- Ursino, M., Zohar, S., Lentz, F., Alberti, C., Friede, T., Stallard, N., and Comets, E. (2017). Dose-finding methods for phase I clinical trials using pharmacokinetics in small populations. *Biometrical Journal*, 59(4):804–825.
- US Food and Drug Administration (2023). Optimizing the Dosage of Human Prescription Drugs and Biological Products for the Treatment of Oncologic Diseases. <https://www.fda.gov/regulatory-information/search-fda-guidance-documents/optimizing-dosage-human-prescription-drugs-and-biological-products-treatment-oncologic-diseases>.
- Whitehead, J., Patterson, S., Webber, D., Francis, S., and Zhou, Y. (2001). Easy-to-implement Bayesian methods for dose-escalation studies in healthy volunteers. *Biostatistics*, 2(1):47–61.
- Whitehead, J., Zhou, Y., Hampson, L., Ledent, E., and Pereira, A. (2007). A Bayesian approach for dose-escalation in a phase I clinical trial incorporating pharmacodynamic endpoints. *Journal of Biopharmaceutical statistics*, 17(6):1117–1129.
- Yuan, Z., Chappell, R., and Bailey, H. (2007). The continual reassessment method for multiple toxicity grades: a Bayesian quasi-likelihood approach. *Biometrics*, 63(1):173–179.

Appendices

Appendix A Prior on ϕ

A.1 Hypergeometric Function

For any value $\phi > 1$, there is a closed form for (8) theoretically (Abramowitz and Stegun, 1968, Ch. 15), which can be represented by

$$\eta(d) = C(d)E_{\max} \int_{\lambda_k}^{\infty} \frac{1}{x^{\phi} + C(d)} dx = C(d)E_{\max} \times \left(\frac{x}{C(d)} F\left(1, \frac{1}{\phi}; 1 + \frac{1}{\phi}; -\frac{x^{\phi}}{C(d)}\right) \right) \Big|_{\lambda_k}^{\infty}.$$

Here, $F(a, b; c; z)$ denotes the Gaussian hypergeometric function.

$$F(a, b; c; z) = \sum_{n=0}^{\infty} \frac{(a)_n (b)_n}{(c)_n} \frac{z^n}{n!} = 1 + \frac{ab}{c} \frac{z}{1!} + \frac{a(a+1)b(b+1)}{c(c+1)} \frac{z^2}{2!} + \dots \quad (\text{A.1})$$

An integral representation of (A.1) is

$$F(a, b; c; z) = \frac{\Gamma(c)}{\Gamma(b)\Gamma(c-b)} \int_0^1 t^{b-1} (1-t)^{c-b-1} (1-tz)^{-a} dt, \quad c > b > 0.$$

Therefore, we can find

$$\begin{aligned} \frac{\partial}{\partial x} \left(\frac{x}{C(d)} F\left(1, \frac{1}{\phi}; 1 + \frac{1}{\phi}; -\frac{x^{\phi}}{C(d)}\right) \right) &= \frac{\partial}{\partial x} \left(\frac{x}{C(d)} \times \frac{1}{\phi} \int_0^1 t^{\frac{1}{\phi}-1} \left(1 + \frac{tx^{\phi}}{C(d)}\right)^{-1} dt \right) \\ &= \frac{\partial}{\partial x} \left(\frac{x}{C(d)} \times \int_0^1 \frac{C(d)}{C(d) + (t^{\frac{1}{\phi}} x)^{\phi}} dt^{\frac{1}{\phi}} \right) \\ &\stackrel{s=t^{\frac{1}{\phi}} x}{=} \frac{\partial}{\partial x} \left(\int_0^x \frac{1}{C(d) + s^{\phi}} ds \right) \\ &= \frac{1}{x^{\phi} + C(d)} \end{aligned}$$

By calling the functions in the GNU Scientific Library of computing the values of (A.1), the MCMC algorithm is achievable with a continuous prior distribution on ϕ or γ in (8). However, the computation of the hypergeometric function is difficult to implement in JAGS, by which our simulation code is written mainly.

A.2 Categorical Prior

For simplicity, we assume a categorical prior distribution on ϕ , $\phi \sim \text{Cat}(4, \mathbf{p})$, where $\phi \in \{2, 3, 4, 5\}$ and $\mathbf{p} = (0.25, 0.25, 0.25, 0.25)$. These values of ϕ result in distinct closed forms for $\eta(d)$.

When $\phi = 2$,

$$\eta(d) = \sqrt{C(d)} E_{\max} \left[\frac{\pi}{2} - \arctan \left(\frac{\lambda_k}{\sqrt{C(d)}} \right) \right].$$

When $\phi = 3$,

$$\begin{aligned}\eta(d) &= \frac{1}{6}C(d)^{\frac{1}{3}}E_{\max} \times \left[2\log\left(C(d)^{\frac{1}{3}} + x\right) - \log\left(C(d)^{\frac{2}{3}} - C(d)^{\frac{1}{3}}x + x^2\right) + 2\sqrt{3}\arctan\left(\frac{2x - C(d)^{\frac{1}{3}}}{\sqrt{3}C(d)^{\frac{1}{3}}}\right) \right] \Big|_{\lambda_k}^{\infty} \\ &= \frac{1}{6}C(d)^{\frac{1}{3}}E_{\max} \times \left[\sqrt{3}\pi - 2\log\left(C(d)^{\frac{1}{3}} + \lambda_k\right) + \log\left(C(d)^{\frac{2}{3}} - C(d)^{\frac{1}{3}}\lambda_k + \lambda_k^2\right) - 2\sqrt{3}\arctan\left(\frac{2\lambda_k - C(d)^{\frac{1}{3}}}{\sqrt{3}C(d)^{\frac{1}{3}}}\right) \right].\end{aligned}$$

When $\phi = 4$,

$$\begin{aligned}\eta(d) &= \frac{1}{4\sqrt{2}}C(d)^{\frac{1}{4}}E_{\max} \times \left[\log\left(x^2 + \sqrt{2}C(d)^{\frac{1}{4}}x + \sqrt{C(d)}\right) - \log\left(x^2 - \sqrt{2}C(d)^{\frac{1}{4}}x + \sqrt{C(d)}\right) \right. \\ &\quad \left. + 2\arctan\left(\frac{\sqrt{2}x}{C(d)^{\frac{1}{4}}} - 1\right) + 2\arctan\left(\frac{\sqrt{2}x}{C(d)^{\frac{1}{4}}} + 1\right) \right] \Big|_{\lambda_k}^{\infty} \\ &= \frac{1}{4\sqrt{2}}C(d)^{\frac{1}{4}}E_{\max} \times \left[\pi - \log\left(\lambda_k^2 + \sqrt{2}C(d)^{\frac{1}{4}}\lambda_k + \sqrt{C(d)}\right) + \log\left(\lambda_k^2 - \sqrt{2}C(d)^{\frac{1}{4}}\lambda_k + \sqrt{C(d)}\right) \right. \\ &\quad \left. - 2\arctan\left(\frac{\sqrt{2}\lambda_k}{C(d)^{\frac{1}{4}}} - 1\right) - 2\arctan\left(\frac{\sqrt{2}\lambda_k}{C(d)^{\frac{1}{4}}} + 1\right) \right].\end{aligned}$$

When $\phi = 5$,

$$\begin{aligned}\eta(d) &= \frac{1}{20}C(d)^{\frac{1}{5}}E_{\max} \times \left[(\sqrt{5} - 1)\log\left(2x^2 + (\sqrt{5} - 1)C(d)^{\frac{1}{5}}x + 2C(d)^{\frac{2}{5}}\right) \right. \\ &\quad - (\sqrt{5} + 1)\log\left(2x^2 + (\sqrt{5} + 1)C(d)^{\frac{1}{5}}x + 2C(d)^{\frac{2}{5}}\right) + 4\log\left(C(d)^{\frac{1}{5}} + x\right) \\ &\quad + 2\sqrt{10 + 2\sqrt{5}}\arctan\left(\frac{4x + (\sqrt{5} - 1)C(d)^{\frac{1}{5}}}{\sqrt{10 + 2\sqrt{5}}C(d)^{\frac{1}{5}}}\right) \\ &\quad \left. + 2\sqrt{10 - 2\sqrt{5}}\arctan\left(\frac{4x - (\sqrt{5} + 1)C(d)^{\frac{1}{5}}}{\sqrt{10 - 2\sqrt{5}}C(d)^{\frac{1}{5}}}\right) \right] \Big|_{\lambda_k}^{\infty} \\ &= \frac{1}{20}C(d)^{\frac{1}{5}}E_{\max} \times \left[\left(\sqrt{10 + 2\sqrt{5}} + \sqrt{10 - 2\sqrt{5}} \right) \pi - (\sqrt{5} - 1)\log\left(2\lambda_k^2 + (\sqrt{5} - 1)C(d)^{\frac{1}{5}}\lambda_k + 2C(d)^{\frac{2}{5}}\right) \right. \\ &\quad + (\sqrt{5} + 1)\log\left(2\lambda_k^2 + (\sqrt{5} + 1)C(d)^{\frac{1}{5}}\lambda_k + 2C(d)^{\frac{2}{5}}\right) - 4\log\left(C(d)^{\frac{1}{5}} + \lambda_k\right) \\ &\quad - 2\sqrt{10 + 2\sqrt{5}}\arctan\left(\frac{4\lambda_k + (\sqrt{5} - 1)C(d)^{\frac{1}{5}}}{\sqrt{10 + 2\sqrt{5}}C(d)^{\frac{1}{5}}}\right) \\ &\quad \left. - 2\sqrt{10 - 2\sqrt{5}}\arctan\left(\frac{4\lambda_k - (\sqrt{5} + 1)C(d)^{\frac{1}{5}}}{\sqrt{10 - 2\sqrt{5}}C(d)^{\frac{1}{5}}}\right) \right].\end{aligned}$$

After collecting data \mathcal{D}_I from Phase I, the posterior distributions of ϕ in the four scenarios of Simulation 1 (Section 4.2) are reported in Table A.1.

Table A.1: Average posterior probabilities of ϕ in the four scenarios of Simulation 1, averaged across 1,000 simulated trials. “Average MAP” denotes the average posterior mode of ϕ across 1,000 simulations. The true ϕ value is 2 in the simulation.

	Average $\Pr(\phi = x \mid \mathcal{D}_1)$				Average
	2	3	4	5	MAP
Sc 1	0.403	0.232	0.129	0.235	2.887
Sc 2	0.47	0.237	0.116	0.177	2.467
Sc 3	0.525	0.239	0.105	0.131	2.277
Sc 4	0.504	0.235	0.11	0.151	2.367